

Evaluation of the performance of $\Delta\phi$ as a precipitation estimator

Author: Ignacio Cordova Pou

Facultat de Física, Universitat de Barcelona, Diagonal 645, 08028 Barcelona, Spain.

Advisor: Dr. Ramon Padullès

(Dated: April 18, 2022)

Abstract: This paper introduces the application of statistical models to determine the performance of the observable $\Delta\phi$ as a precipitation estimator. Using Precision Recall curves, the study shows the optimal range of heights for transforming the vertical profiles of $\Delta\phi$ into a scalar average. The results show that Using NASA's IMERG precipitation data as our target with the 97th percentile mm/h as True, $\Delta\phi$ achieves an optimal F1 score of 0.54 when averaged between 0.1km and 8.5km.

I. INTRODUCTION

A Global Navigation Satellite System (GNSS) radio occultation (RO) experiment is taking place in the Spanish low Earth orbiter PAZ satellite. The RO payload provides globally distributed vertical profiles of the atmosphere which have been proven to have a high impact on Numerical Weather Prediction Models[referencia]. Moreover, the mission runs for the first time a double-polarization GNSS RO experiment for detecting precipitation events. The performance of this new technique, which has already been proven to be successful, is evaluated in this paper.

The GNSS systems transmit circular-polarized signals that are collected using ROs after having travelled through the atmosphere. They are collected using two orthogonal linearly polarized antennas (horizontal H and vertical V) with the aim of comparing the phase delay ϕ_H and ϕ_V . In the case of heavy rain events, water drops experience air friction which causes them to flatten out along their horizontal dimension. The presence of water drops can cause depolarization between the H and V signals which are affected differently when propagating through a rainy atmosphere. The polarimetric radio occultations (PROs) is a new technique that allows us to measure the differential phase shift $\Delta\phi$ between the H and V signals. One of the objectives of the ROHP-PAZ mission is to use the measured depolarization $\Delta\phi$ as a precipitation estimator.

This paper evaluates the performance of $\Delta\phi$ on detecting precipitation events. To properly evaluate the performance a target must be defined. The target used in this paper is the NASA's IMERG precipitation dataset. From this dataset we can obtain the precipitation in mm/h at every location in time and space where our PROs took place. The goal is to evaluate and quantify how well does the $\Delta\phi$ estimator perform in detecting precipitation above a certain threshold regarded as *true precipitation*. This way, **our target is defined as a binary True/False variable** being True for precipitation above the elected threshold and False for precipitation below it.

Our array-like observable is of little use to the Numer-

ical Weather Prediction Models. This study provides the optimal range of heights $[h_o, h_f]$ for transforming the vertical profiles of $\Delta\phi$ into a scalar average. This optimal range depends on the threshold used to binarize our *true precipitation* and, as found in this study, on the region where the PRO took place. The performance of each average $[h_o, h_f]$ is evaluated using Precision-Recall curves which have been proven to work well with unbalanced datasets [reference]. In our case, the target False (no precipitation event) will outnumber the target True once a proper truth threshold is defined.

It is expected that the average $[h_o, h_f]$ that best predicts the True/False target will be somewhere between 0.1km and 10.0km since that is where the signal will experience the most depolarization.

II. DATA

The data collected by the PAZ satellite are downlinked by Hisdesat. The Institut de Ciències de l'Espai (ICE), Consejo Superior de Investigaciones Científicas, Institut d'Estudis Espacials de Catalunya (CSIC, IEEC) collects and owns the data and provides access to the servers at the Jet Propulsion Laboratory (JPL). At the JPL, the raw data are processed and converted to level 1 RO products, which are finally analyzed.

The main observable of the experiment is the differential phase shift

$$\Delta\phi = \phi_H - \phi_V, \quad (1)$$

The dataset is composed of over 85.000 measurements distributed globally providing vertical profiles of $\Delta\phi$ in 100m intervals between 0.1km and 40km. A *true precipitation* is associated with each of these measurements. As an example, 1 measurement is shown below:

You can insert equations in the text, like $e^{i\pi} + 1 = 0$; $\frac{df(x)}{dx}$ or you may prefer $\frac{df(x)}{dx}$. You can also write aligned

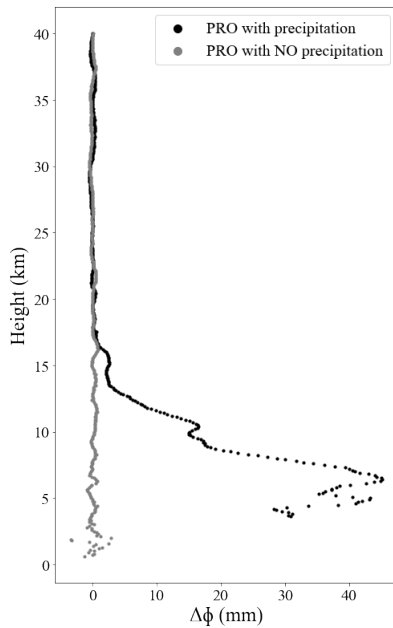


FIG. 1: A sample figure.

equations,

$$\begin{aligned} \frac{du(x)}{dx} + Vu(x) + Wv(x) &= (\lambda + \alpha) u(x) \\ \frac{dv(x)}{dx} + Vv(x) + Wu(x) &= (\lambda - \alpha) v(x). \end{aligned} \quad (2)$$

Further examples are,

$$\begin{aligned} \nabla \cdot \vec{E} &= 4\pi\rho \\ \nabla \times \vec{B} - \frac{1}{c} \frac{\partial \vec{E}}{\partial t} &= \frac{4\pi}{c} \vec{J} \\ \nabla \times \vec{E} + \frac{1}{c} \frac{\partial \vec{B}}{\partial t} &= 0 \\ \nabla \cdot \vec{E} &= 0, \end{aligned} \quad (3)$$

as can be found in [?], pag. 14. Also,

$$E = -J \sum_{i=1}^N s_i s_{i+1}. \quad (4)$$

You can define your own macros to save typing [?]. For example, suppose that you introduce a macro as follows:

```
\newcommand{\E1}{\vec{E}(\vec{x},t)}
```

Then, by simply typing,

```
\E1
```

you get the electric field $\vec{E}(\vec{x}, t)$ printed out (in math mode, of course).

You can write \tilde{x} , \bar{A} ; %, accents: Schrödinger and é, à,

À, Martí; calçotada, $A \equiv B$, $\vec{A} \cdot \vec{B}$, $\vec{A} \times \vec{B}$, \vec{v} , \hat{n} , $c \sim d$, $z \approx w$, $\langle x \rangle$, $\langle \psi | X | \psi \rangle$, \hbar , g_{ij} , δ_j^i , $R_{\mu\nu\alpha\beta;\xi}$.

You can also quote references easily, i.e., [?], [?].

A matrix

$$\begin{pmatrix} 0 & 1 & 0 \\ 1 & 0 & 1 \\ 0 & 1 & 0 \end{pmatrix}, \quad (5)$$

a vector (column)

$$\begin{pmatrix} 1 \\ \sqrt{3} \\ \pi \end{pmatrix}, \quad (6)$$

a row,

$$(p \ q \ r), \quad (7)$$

and a determinant,

$$\begin{vmatrix} a_{11} & a_{12} & a_{13} \\ a_{21} & a_{22} & a_{23} \\ a_{31} & a_{32} & a_{33} \end{vmatrix}. \quad (8)$$

Further examples:

$$\int_{-\infty}^{\infty} e^{-x^2} dx = \sqrt{\pi}, \quad (9)$$

also,

$$\int_a^b f'(x) dx = f(b) - f(a), \quad (10)$$

and so on.

A. Tables and figures

An example of a table is shown in Table ??.

TABLE I: Force, area, and pressure data for an experiment with glass syringes.

	Piston 1	Piston 2
Force (N)	4.40	2.25
Area (cm ²)	6.16	3.14
Pressure (N/cm ²)	0.714 ± 0.002	0.716

Here we try to insert an illustrating figure, Fig. ??. For that you need to have created the figure before, in this case the fig1.pdf file.



FIG. 2: A sample figure.

III. DEVELOPING SECTIONS

TABLE II: Another table.

M1 (11:45)	Teoria:	Galileo	A11G
	Problemes:	Newton	A11G
(12:45)	Problemes	Planck (M1A)	A11G
	tutoritzats:	Fermi (M1B)	A23M
M2 (8:30)	Teoria:	Clausius	A12G
	Problemes:	Goeppert Mayer	A12G
(9:30)	Problemes	Boltzmann (M2A)	A12G
	tutoritzats:	Maxwell (M2B)	A24M
T1 (18:00)	Teoria:	Gibbs	A12G
	Problemes:	Helmholtz	A12G
(19:00)	Problemes	Bohr (T1A)	A12G
	tutoritzats:	Einstein (T1B)	A24M

[illegible]

This is the first subsection.

[illegible]

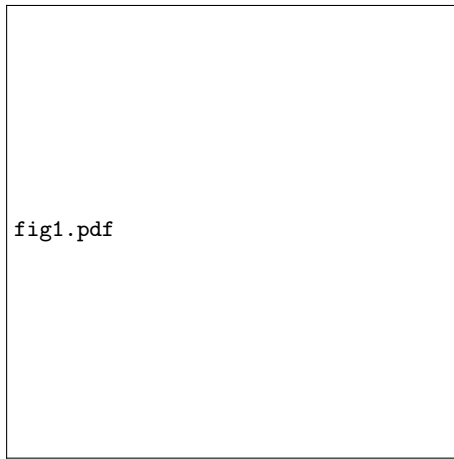


FIG. 3: A sample figure made smaller by changing the width parameter.

B. Subsection 2

IV. CONCLUSIONS

- is important in Physics.
-
-
-
-
-
-
-
-
- .

V. APPENDIX

Acknowledgments

You can add your appendix if needed, or you should like to do so. The following equation,

$$\vec{F} = m\vec{a}, \quad (11)$$

Be sure to thank your advisor, your colleagues, and granting agencies (e.g. parents, etc...) as well.

-
- [1] Helmut Kopka and Patrick W. Daly, *A Guide to L^AT_EX: Document Preparation for Beginners and Advanced Users*, 3rd. ed. (Addison-Wesley, Reading, MA, 1999).
 - [2] It is necessary to process a file twice to get the counters correct.
 - [3] J.D. Jackson, *Classical Electrodynamics*, (John-Wiley & Sons, New York 1975, 2nd. ed.).
 - [4] Hinshaw, G. et al. (WMAP Collaboration). "Five-Year Wilkinson Microwave Anisotropy Probe Observations: Data Processing, Sky Maps, and Basic Results". *The Astrophysical Journal Supplement* **180**: 225–245 (2009).
 - [5] Weinberg, S.. "High-Energy Behavior in Quantum Field Theory". *Phys. Rev.* **118**: 838–849 (1960).
 - [6] This is a footnote.